

# Model for the Production of CO Cameron band emission in Comet 1P/Halley

Susarla Raghuram and Anil Bhardwaj\*

*Space Physics Laboratory, Vikram Sarabhai Space Centre, Trivandrum 695022, India.*

## Abstract

The abundance of CO<sub>2</sub> in comets has been derived using CO Cameron band ( $a^3\Pi \rightarrow X^1\Sigma^+$ ) emission assuming that photodissociative excitation of CO<sub>2</sub> is the main production process of CO( $a^3\Pi$ ). On comet 1P/Halley the Cameron (1-0) band has been observed by International Ultraviolet Explorer (IUE) on several days in March 1986. A coupled chemistry-emission model is developed for comet 1P/Halley to assess the importance of various production and loss mechanisms of CO( $a^3\Pi$ ) and to calculate the intensity of Cameron band emission on different days of IUE observation. Two different solar EUV flux models, EUVAC of Richards et al. (1994) and SOLAR2000 of Tobiska (2004), and different relative abundances of CO and CO<sub>2</sub>, are used to evaluate the role of photon and photoelectron in producing CO molecule in  $a^3\Pi$  state in the cometary coma. It is found that in comet 1P/Halley 60–70% of the total intensity of the Cameron band emission is contributed by electron impact excitation of CO and CO<sub>2</sub>, while the contribution from photodissociative excitation of CO<sub>2</sub> is small (20–30%). Thus, in the comets where CO and CO<sub>2</sub> relative abundances are comparable, the Cameron band emission is largely governed by electron impact excitation of CO, and not by the photodissociative excitation of CO<sub>2</sub> as assumed earlier. Model calculated Cameron band 1-0 emission intensity (40 R) is consistent with the observed IUE slit-averaged brightness ( $37 \pm 6$  R) using EUVAC model solar flux on 13 March 1986, and also on other days of observations. Since electron impact excitation is the major production mechanism, the Cameron emission can be used to derive photoelectron density in the inner coma rather than the CO<sub>2</sub> abundance.

**Keywords:** CO molecule, comet 1P/Halley, Cameron band emission, UV emission, photochemistry

## 1. Introduction

Ejecting neutral gas and dust into space, comets create extensive and unique atmospheres in the interplanetary space. Interaction of solar extreme ultraviolet (EUV) radiation with cometary species causes spectrum of different emissions. Spectroscopic observations of comets in the UV region by space-based telescopes give information about composition, abundance, and spatial distribution of neutral species in the cometary coma (e.g., Feldman et al., 2004). The number densities of CO<sub>2</sub> and CO in cometary coma have been derived using emissions from the dissociative products which can be produced in metastable states. Assuming photodissociative excitation is the main production mechanism in populating the  $a^3\Pi$  metastable state of CO, the Cameron band ( $a^3\Pi \rightarrow X^1\Sigma^+$ ) emission has been used to estimate

the abundance of CO<sub>2</sub> in comets (Weaver et al., 1994; Weaver et al., 1997; Feldman et al., 1997).

The observation of Cameron band of CO molecule in the coma of comet 103P/Hartley 2 (Weaver et al., 1994) by Hubble Space Telescope (HST) gave an incentive to re-examine the data of several comets observed by the International Ultraviolet Explorer (IUE) satellite. Cameron band (1-0) emission at 1993 Å is observed in 4 comets, including comet 1P/Halley, in the IUE spectra (Feldman et al., 1997). The Cameron band (0-0) and (0-1) emissions at 2063 and 2155 Å, respectively, could not be observed since they fall in the low sensitivity end of the IUE long-wavelength camera. Since the excited upper state ( $a^3\Pi$ ) of Cameron band emission is metastable and its lifetime is very small (~3 ms, Gilijamse et al., 2007) compared to lifetime of CO<sub>2</sub> molecule (~135 hours at 1 AU, Huebner et al., 1992), the CO( $a^3\Pi$ ) molecule can travel a distance of few meters only in the cometary coma before de-exciting into ground state ( $X^1\Sigma^+$ ) via emitting photons. Hence, the

\*Corresponding author: anil.bhardwaj@vssc.gov.in, bhardwaj\_spl@yahoo.com

Cameron band emission can be used to probe CO<sub>2</sub> distribution, and thus its abundance in the coma, provided it is produced only through photodissociation of CO<sub>2</sub>.

Besides photons, the solar EUV-generated photoelectrons also play a significant role in driving the chemistry of cometary species in the coma. The importance of photoelectrons in excitation, dissociation, and ionization of various cometary species and subsequent effects on emissions in the inner coma are discussed in several works (e.g., Cravens and Green, 1978; Ip, 1985; Boice et al., 1986; Körösmezey et al., 1987; Bhardwaj et al., 1990, 1996; Haider et al., 1993; Häberli et al., 1996; Bhardwaj, 1999, 2003; Haider and Bhardwaj, 2005; Campbell and Brunger, 2009; Feldman et al., 2009; Bhardwaj and Raghuram, 2011a,b). To explain the Cameron band emission in comet 103P/Hartley 2, Weaver et al. (1994) considered five possible production mechanisms of CO(*a*<sup>3</sup>Π) molecule. The modelled Cameron band emission of CO molecule by Weaver et al. (1994) suggested that 60% of total CO(*a*<sup>3</sup>Π) production can be through photodissociative excitation of CO<sub>2</sub>; the remaining was attributed to other excitation processes. Feldman et al. (1997) assumed that photodissociative excitation of CO<sub>2</sub> is the only source of Cameron band emission in comet 1P/Halley. Recent calculations of Bhardwaj and Raghuram (2011a) have demonstrated that in the comet 103P/Hartley 2, 60 to 90% of CO(*a*<sup>3</sup>Π) production is through the photoelectron impact of CO<sub>2</sub> and CO and that the contribution of photodissociation of CO<sub>2</sub> is quite small. The derived rates of electron impact dissociation of CO<sub>2</sub> producing CO(*a*<sup>3</sup>Π) by Feldman et al. (2009) show that photodissociation can be comparable with electron impact excitation in producing Cameron band emission. However, the comet 103P/Hartley 2 is depleted in CO (relative abundance <1%). But in the case of comet 1P/Halley the CO abundance is relatively higher compared to that on the 103P/Hartley 2, and hence the contribution due to direct excitation of CO by electron impact would be much larger.

There are several observations of CO in comet 1P/Halley, as well as in other comets, which suggest that CO is produced directly from the nucleus as well as having prevailed distributed sources in the cometary coma (Eberhardt et al., 1987; Eberhardt, 1999; DiSanti et al., 2003; Cottin and Fray, 2008). The measured number density of CO by neutral mass spectrometer on Giotto spacecraft, which flew through the coma of 1P/Halley, is ≤7% relative to water at 1000 km cometocentric distance. This relative abundance is higher (≤15%) at larger distances ( $2 \times 10^4$  km) in the coma (Eberhardt et al., 1987; Eberhardt, 1999; Festou, 1999).

This increase in abundance can be explained by dissociation of CO-bounded species and also through heating of several refractory grains by sunlight. Other cometary species like H<sub>2</sub>CO, C<sub>3</sub>O<sub>2</sub>, POM (polyoxymethylene, or polyformaldehyde), CH<sub>3</sub>OH, and CO<sub>2</sub> can also produce CO molecules in photodissociation process (see Greenberg and Li, 1998; Cottin and Fray, 2008, and references there in). However, there are no literature reports on the production of CO(*a*<sup>3</sup>Π) from CO-bearing species, like H<sub>2</sub>CO, CH<sub>3</sub>OH, and C<sub>3</sub>O<sub>2</sub>, via photodissociation or electron impact dissociative excitation.

Reanalysis of the IUE data on comet 1P/Halley showed 5 observations of the Cameron 1-0 band emission, which span over a 10-days period in March 1986; the intensity of 1-0 emission varied by a factor of about 4 from lowest value of  $20 \pm 6$  to highest value of  $65 \pm 9$  Rayleighs (Feldman et al., 1997). Assuming that the production of Cameron band emission is only through photodissociation of CO<sub>2</sub>, Feldman et al. (1997) derived the CO<sub>2</sub> abundances of ~2 to 6%, and also the CO<sub>2</sub>/CO abundance ratio.

The production of CO(*a*<sup>3</sup>Π) is mainly associated with spatial distribution of CO<sub>2</sub> and CO molecules in the coma. We have recently developed a model for the chemistry of CO(*a*<sup>3</sup>Π) on comet 103P/Hartley 2 (Bhardwaj and Raghuram, 2011a). In the present paper this coupled chemistry model has been employed to study the production of Cameron band emissions on comet 1P/Halley. The contributions of major production and loss processes of CO(*a*<sup>3</sup>Π) in comet 1P/Halley are evaluated for different relative abundances of CO and CO<sub>2</sub>.

The photochemistry in the cometary coma is driven by solar UV-EUV radiation. The solar UV flux is known to vary considerably both with the 27-day solar rotation period and with the 11-year solar activity cycle. Since the continuous measurements of solar EUV fluxes are not available for different cometary observations, one has to depend on the empirical solar EUV models. To assess the impact of solar EUV flux on the calculated brightness of Cameron band emission we have taken two most commonly used solar EUV flux models, namely EUVAC model of Richards et al. (1994) and SOLAR2000 v.2.3.6 (S2K) model of Tobiska (2004). The solar EUV flux from these two models for 13 March 1986 are shown in Fig. 1.

This paper will demonstrate that in comets where CO<sub>2</sub> and CO relative abundances are comparable, the photoelectron impact excitation of CO plays a major role in controlling the brightness of Cameron band, and not the photodissociation of CO<sub>2</sub> as assumed previously. Since the Cameron band emission is forbidden and electron impact is the major excitation mechanism, this

emission is suitable to track photoelectron flux in the inner cometary coma rather than the CO<sub>2</sub> abundance. We have also studied the sensitivity of calculations associated with variation in input solar flux and electron impact excitation cross sections of CO<sub>2</sub> and CO in estimating the intensity of Cameron band emission.

## 2. Model

The neutral parent species considered in the model are H<sub>2</sub>O, CO<sub>2</sub>, and CO. The density of neutral parent species in the coma is calculated using Haser's formula, which assumes spherical distribution of gaseous environment around the nucleus. The number density  $n_i(r)$  of  $i^{th}$  species in the coma at a cometocentric distance  $r$  is given by

$$n_i(r) = \frac{f_i Q_p}{4\pi v_i r^2} (e^{-\beta_i/r}) \quad (1)$$

Here  $Q_p$  is the total gas production rate of the comet,  $v_i$  is the average velocity of neutral species taken as 1 km s<sup>-1</sup>,  $\beta_i$  is scale length ( $\beta_{H_2O} = 8.2 \times 10^4$  km,  $\beta_{CO_2} = 5.0 \times 10^5$  km, and  $\beta_{CO} = 1.4 \times 10^6$  km) and  $f_i$  is fractional abundance of  $i^{th}$  species. Calculations are made for comet 1P/Halley taking total gas production rate as  $6.9 \times 10^{29}$  s<sup>-1</sup>, which has been observed by Giotto mission (Krankowsky et al., 1986). Since cometary coma is dominated by water, 80% of total production rate is assumed to be H<sub>2</sub>O.

The in situ gas measurements at comet 1P/Halley made by Giotto Neutral Mass Spectrometer (NMS) on the encounter date 13 March 1986 showed that CO<sub>2</sub> abundance is 3.5% of water (Krankowsky et al., 1986). On the same day, based on IUE observation, Feldman et al. (1997) derived CO<sub>2</sub> abundance of 4.3%. Eberhardt et al. (1987) suggested that below 1000 km, nuclear rate of CO production can be 7% of water. The radial profile of CO calculated by Eberhardt et al. (1987) showed almost a constant value of CO relative abundance ( $\leq 15\%$ ) above 15000 km. This increase in CO abundance is attributed to the presence of an extended source for CO in the cometary coma. The IUE-derived average production rate of CO is 4.7% (Feldman et al., 1997). We have taken 4% CO<sub>2</sub> and 7% CO directly coming from nucleus as the standard input for the model. We have also considered extended CO density profile directly from Giotto NMS observation (Eberhardt et al., 1987). Further, the relative abundances of CO<sub>2</sub> and CO are varied to assess the effect on the intensity of Cameron band emission and different production channels of CO(a<sup>3</sup>Π).

The primary photoelectron energy spectrum  $Q(E, r, \theta)$ , at energy  $E$ , cometocentric distance  $r$ ,

and solar zenith angle  $\theta$ , is calculated by degrading the solar UV-EUV radiation in the cometary coma using the following equation

$$Q(E, r, \theta) = \sum_i \int_{\lambda} n_i(r) \sigma_i^I(\lambda) I_{\infty}(\lambda) \exp[-\tau(r, \theta, \lambda)] d\lambda \quad (2)$$

where,

$$\tau(r, \theta, \lambda) = \sum_i \sigma_i^A(\lambda) \sec\theta \int_r^{\infty} n_i(r') dr' \quad (3)$$

Here  $\sigma_i^A(\lambda)$  and  $\sigma_i^I(\lambda)$  are absorption and ionization cross sections, respectively, of  $i^{th}$  species at wavelength  $\lambda$ ,  $n_i(r)$  is its neutral gas density calculated using the equation 1, and  $\tau(r, \theta, \lambda)$  is optical depth of the medium.  $I_{\infty}(\lambda)$  is unattenuated solar flux at the top of atmosphere at wavelength  $\lambda$ . All calculations are made at solar zenith angle 0°. The photoabsorption and photoionization cross sections of H<sub>2</sub>O, CO<sub>2</sub>, and CO are taken from Shunk and Nagy (2009).

The steady state photoelectron fluxes are calculated using the Analytical Yield Spectrum (AYS) approach, which is based on the Monte Carlo method. Details of the AYS approach are given in several of the previous papers (Singhal and Haider, 1984; Bhardwaj et al., 1990, 1996; Singhal and Bhardwaj, 1991; Bhardwaj and Singhal, 1993; Bhardwaj, 1999, 2003; Bhardwaj and Michael, 1999a,b; Haider and Bhardwaj, 2005; Bhardwaj and Jain, 2009). We have used two dimensional yield spectra to calculate photoelectron flux  $f_p(E, r)$  as a function of energy  $E$  and cometocentric distance  $r$

$$f_p(E, r) = \int_w^{\infty} \frac{Q(E, r, \theta) U^c(E, E_o)}{\sum_i n_i(r) \sigma_{iT}(E)} dE \quad (4)$$

where  $Q(E, r, \theta)$  is primary photoelectron production rate calculated using equation 2.  $\sigma_{iT}(E)$  is total inelastic electron impact cross section at energy  $E$  for the  $i^{th}$  species whose number density is  $n_i(r)$ . The lower limit of integration  $w$  is minimum excitation energy and  $U^c(E, E_o)$  is two dimensional composite yield spectra (Singhal and Haider, 1984; Bhardwaj et al., 1990). The total inelastic electron impact cross sections for water are taken from Rao et al. (1995), and those for CO<sub>2</sub> and CO are taken from Jackman et al. (1977).

The loss process of photoelectrons through collisions with thermal electrons is considered using the following formula

$$n_e \sigma_{e-e}^{eff} = \frac{n_e \beta(E, n_e, T)}{E \bar{W}} \quad (5)$$

where  $n_e$  is the thermal electron density,  $E$  is the energy of photoelectron, and  $\bar{W}$  is the average energy lost per

collision between photoelectron and the thermal electron. The expression  $\beta$  is given by McCormick et al. (1976). More details are provided in Bhardwaj et al. (1990). The calculated photoelectron fluxes for the two solar EUV flux models at 1000 km are shown in Fig. 2.

The electron impact volume production rates of different ions from neutral species and volume excitation rates for CO( $a^3\Pi$ ) state from CO<sub>2</sub> and CO are calculated using photoelectron flux  $f_p(E, r)$  and electron impact excitation cross section  $\sigma_{ik}$  of  $i^{th}$  species and  $k^{th}$  state as

$$V(r) = n_i(r) \int_w^{100} f_p(E, r) \sigma_{ik}(E) dE \quad (6)$$

The cross sections for electron impact dissociative ionization of water are taken from Itikawa and Mason (2005), for CO<sub>2</sub> from Bhardwaj and Jain (2009), and for CO from McConkey et al. (2008).

Table 1 presents the reactions involved in the production and loss of CO( $a^3\Pi$ ). Huebner et al. (1992) calculated the cross section for photodissociative excitation of CO<sub>2</sub> producing CO in  $a^3\Pi$  state using total absorption cross section and the yield measured by Lawrence (1972). We averaged these cross section values over 50 Å bin intervals to calculate photodissociative excitation rate using solar flux from EUVAC and S2K models; this cross section is shown in Fig. 3. The cross section for electron impact excitation of CO in the  $a^3\Pi$  state is taken from Jackman et al. (1977) and for dissociative excitation of CO<sub>2</sub> producing CO( $a^3\Pi$ ) is taken from Bhardwaj and Jain (2009). These cross sections are presented in Fig. 2. To estimate the effect of electron impact cross sections on emissions, we have used the electron impact cross sections recommended by Avakyan et al. (1998) for the above two processes, which are also shown in Fig. 2. The electron temperature profile, required for dissociative recombination reactions, is taken from Körösmezey et al. (1987).

### 3. Results and discussions

#### 3.1. Cameron band emission

The first clear observation of Cameron band emission of CO molecule is made in comets 103P/Hartley 2 and C/1992 T2 Shoemaker-Levy (Weaver et al., 1994), which was followed by detection in several other comets, including 1P/Halley, in the IUE reprocessed data (Feldman et al., 1997). Assuming that the photodissociative excitation of CO<sub>2</sub> is the major production mechanism of Cameron band emission, Weaver et al. (1994) derived the abundance of CO<sub>2</sub>

in comet 103P/Hartley 2. Recently, Bhardwaj and Raghuram (2011a) have demonstrated that on comet 103P/Hartley 2 the photoelectron impact dissociative excitation of CO<sub>2</sub> followed by photoelectron impact of CO are the major production processes of Cameron band, and not the photodissociative excitation of CO<sub>2</sub> as suggested by Weaver et al. (1994).

Since comet 103P/Hartley 2 is CO depleted (relative abundance  $\leq 1\%$ ), the contribution to Cameron band emission through dissociative excitation of CO<sub>2</sub> by EUV-generated photoelectrons is more important. However, in case of comets where CO abundance is larger, like 1P/Halley, the contribution of CO to the Cameron band emission would be significant. The derived CO<sub>2</sub>/CO abundance ratios for several IUE observations of comet 1P/Halley showed that the abundance of CO can be even double that of CO<sub>2</sub> (Feldman et al., 1997).

The calculated production rate profiles of CO( $a^3\Pi$ ) using solar EUVAC and S2K models for relative abundance of 4% CO<sub>2</sub> and 7% CO are shown in Figure 4. For both solar EUV flux models, the peak production rate occurs at cometocentric distance  $\sim 20$  km. The major production mechanism of CO( $a^3\Pi$ ) is the photoelectron impact of CO, whose contribution is  $\sim 70\%$  to the total CO( $a^3\Pi$ ) production. On using the S2K solar flux, the calculated total production rate is 1.5 times larger than that obtained using the EUVAC flux. This variation is mainly due to the difference in the input solar EUV flux (cf. Fig. 1) and subsequently EUV-generated photoelectron flux (cf. Fig. 2). In the wavelength region 700–1050 Å, the S2K model solar flux is a factor of  $\sim 2.5$  larger than the EUVAC model (cf. Fig. 1). As shown in Figure 3, the photodissociative excitation cross section of CO<sub>2</sub> producing CO( $a^3\Pi$ ) maximizes around 880–1000 Å. Further, the S2K solar flux in the 1000–1050 Å wavelength bin is around 20 times higher than the EUVAC flux. The average cross section value for photodissociation of CO<sub>2</sub> producing CO( $a^3\Pi$ ) in the wavelength region 1000–1050 Å is comparable with the peak value around 900 Å (cf. Figure 3).

Moreover, in the inner cometary coma, below cometocentric distance of 50 km, the optical depth for solar flux at wavelengths below 200 Å and above 1000 Å is smaller compared to other wavelengths because of smaller absorption cross sections of neutral species (mainly water). The rate of photodissociative excitation of CO<sub>2</sub> molecule into CO( $a^3\Pi$ ) mainly depends on the degradation of solar flux in the wavelength region 850–1050 Å. Hence, in the innermost coma ( $\leq 50$  km), for a given relative abundance of CO<sub>2</sub>, the production rate of CO( $a^3\Pi$ ) via photodissociation of CO<sub>2</sub> is determined

by the solar flux in the wavelength bin 1000–1050 Å and at wavelengths 1025.7 Å (H I) and 1031.9 Å (O VI). The calculated photodissociation rates of CO<sub>2</sub> producing CO(a<sup>3</sup>Π) at 0.9 AU are  $1.66 \times 10^{-7} \text{ s}^{-1}$  and  $5.28 \times 10^{-7} \text{ s}^{-1}$  using EUVAC and S2K solar fluxes, respectively, on 13 March 1986.

From Figure 2 it is seen that the calculated steady state photoelectron flux using two solar flux models differ in magnitude by a factor of 2. Since the cross section for electron impact of CO producing CO(a<sup>3</sup>Π) peaks at lower energies (~10 eV) where the photoelectron flux is also high (~ $10^8 \text{ cm}^{-2} \text{ s}^{-1} \text{ eV}^{-1} \text{ sr}^{-1}$ ; cf. Fig. 2), the electron impact excitation of CO is a major production source of Cameron band emission. At larger (>5000 km) cometocentric distances, due to decrease in photoelectron flux, the photodissociative excitation of CO<sub>2</sub> starts becoming an increasingly important process (cf. Fig. 4). Contributions from dissociative recombination reactions and resonance fluorescence of CO are more than two orders of magnitude lower compared to major production processes.

Since the lifetime of CO(a<sup>3</sup>Π) is about ~3 ms, the quenching of the excited a<sup>3</sup>Π metastable state by various cometary species is not very efficient. The calculated loss rate profiles of CO(a<sup>3</sup>Π) for various processes are shown in Figure 5. The radiative de-excitation is the main loss process. Very close to the nucleus, the loss due to quenching of CO(a<sup>3</sup>Π) by water is comparable to the radiative de-excitation. Quenching by water molecule would be a more significant loss process of CO(a<sup>3</sup>Π) in the higher water production rate comets, like Hale-Bopp or when the comet is much closer to the Sun than 1 AU. The calculated number density profile of CO(a<sup>3</sup>Π) is shown in Fig. 6. Above 100 km, the density profile of CO(a<sup>3</sup>Π) mostly following the number density profiles of the parent species CO<sub>2</sub> and CO.

The above calculated total production rate is integrated up to  $10^5 \text{ km}$  to obtain the height-integrated column intensity of Cameron band emission which is presented in Table 2. We also calculated the line of sight intensity at a given projected distance  $z$  from the cometary nucleus using production rates of different excitation processes of CO(a<sup>3</sup>Π) as

$$I(z) = 2 \int_z^R V(s) ds \quad (7)$$

where  $s$  is abscissa along the line of sight and  $V(s)$  is the corresponding emission rate. The maximum limit of integration  $R$  is taken as  $10^5 \text{ km}$ . These brightness profiles are then averaged over the projected area  $6600 \times 11000 \text{ km}^2$  corresponding to the IUE slit dimension  $9''.07 \times 15''.1$  centred on nucleus of comet 1P/Halley

on 13 March 1986 at geocentric distance 0.96 AU. The volume emission rate for 3 transitions (0-0, 1-0, and 0-1) of the Cameron band are calculated using the following formula

$$V_{\nu'\nu''}(r) = q_{\nu\nu'}(A_{\nu'\nu''} / \sum_{\nu''} A_{\nu'\nu''}) V(r) \exp(-\tau) \quad (8)$$

where  $V(r)$  is total volume excitation rate of CO(a<sup>3</sup>Π) at a given cometocentric distance  $r$ , given by equation 6,  $q_{\nu\nu'}$  is the Franck-Condon factor for transition,  $A_{\nu'\nu''}$  is the Einstein transition probability from upper state  $\nu'$  to lower state  $\nu''$ , and  $\tau$  is the optical depth. Since resonance fluorescence is not an effective excitation mechanism for the Cameron band, the cometary coma can be safely assumed to be optically thin. The Franck-Condon factors are taken from Nicholls (1962) and branching ratios from Conway (1981).

The calculated brightness profiles for each of the production processes along projected distances from nucleus are shown in Figure 7. At 100 km projected distance, the contribution due to photoelectron impact excitation of CO to the total Cameron band intensity is about a factor 4 higher than the dissociative excitation processes of CO<sub>2</sub>, while contributions of other production processes are around 2 orders of magnitude smaller. Around 1000 km projected distance, both photodissociative excitation and electron impact dissociative excitation of CO<sub>2</sub> are contributing equally to the total Cameron band intensity. The photodissociative excitation of CO<sub>2</sub> dominates the electron impact excitation processes above 5000 km.

The calculated relative contributions of (1-0), (0-0), and (0-1) bands to the total Cameron band are 13.9%, 10.4%, and 14.5%, respectively. The intensities of (1-0), (0-0) and (0-1) Cameron bands of CO molecule are calculated as a function of relative abundances of CO<sub>2</sub> and CO. The calculated percentage contributions of different production processes of Cameron band at three projected distances for two different solar flux models are presented in Table 2. The IUE-observed 1-0 Cameron band emission on 13 March 1986 is  $37 \pm 6$  Rayleighs.

Using EUVAC solar flux as input, our model calculated 1-0 Cameron band emission intensity for the relative abundance 4% CO<sub>2</sub> and extended distribution of CO is 59 Rayleighs which is higher than IUE observed intensity by a factor 1.3 to 2. Taking CO<sub>2</sub> abundance as 4% and CO abundance as 7% from nucleus, the calculated 1-0 intensity is 51 Rayleighs, which is higher than the IUE-observed value by a factor 1.2 to 1.6. The calculated intensity for 3% CO<sub>2</sub> and 7% CO

is 46 Rayleighs, which is consistent only with the upper limit of IUE-observed intensity. In all the above cases, below 1000 km projected distances, the contribution of photodissociation of CO<sub>2</sub> to the Cameron band emission is <15%, while electron impact of CO contribute 65 to 80%. We have also calculated the intensity of Cameron band taking the Feldman et al. (1997) derived abundances of 4.3% CO<sub>2</sub> and 4.7% CO. The calculated intensity of 1-0 Cameron band emission in this case is 40 R, which is consistent with the observed value of  $37 \pm 6$  R on 13 March 1986 (cf. Table 3). The calculated 1-0 Cameron band emission intensity at various projected distances in the IUE-slit field of view is presented in the Figure 8; The circular contours and gray scale provide information on brightness variation. The calculated results using S2K solar flux model for the above discussed relative compositions of CO<sub>2</sub> and CO are also presented in Table 2. The calculated intensities are higher by a factor of  $\sim 1.5$ , which is mainly due to higher input solar flux and subsequently EUV-produced photoelectron's flux (cf. Figs. 1 and 2).

Using OH 3085 Å emission observation by IUE, Tozzi et al. (1998) derived water production rates for different days of IUE observations (1986 March 9, 11, 13, 16, 18) around Giotto encounter period. The water production rate derived on 13 March 1986, the closest approach day of Giotto spacecraft, was  $5.9 \times 10^{29}$  s<sup>-1</sup>. Feldman et al. (1997) have considered these derived production rates of H<sub>2</sub>O to estimate relative abundances of CO<sub>2</sub> and CO for corresponding days of observation. We have calculated the intensity of Cameron band for different days of IUE observations taking the same H<sub>2</sub>O, CO<sub>2</sub>, and CO production rates as quoted in Feldman et al. (1997). The solar EUV fluxes on each day of observation was obtained by using EUVAC and S2K solar flux models and scaling them according to the heliocentric distance of comet. The IUE projected field of view is calculated for IUE slit dimension used in observation, which vary according to the geocentric distance of the comet in March 1986. The calculated intensities of Cameron 1-0, 0-0, 0-1 bands and percentage contributions from different production process to the IUE slit-averaged brightness are presented Table 3. The calculated intensity of 1-0 emission is consistent with the IUE-observation for the EUVAC solar flux model, while it is higher by a factor of 1.5 on using S2K solar flux. The calculations presented in Table 3 show that for a change in the CO<sub>2</sub>/CO abundance ratio by a factor of 2, the total photoelectron impact excitation contribution changes by only  $\sim 10\%$ ; it varies from 68 to 76% (60 to 69%) of the total IUE-observed intensity for EUVAC (S2K) solar flux model. The photoelectron

impact excitation of CO alone contribute around 45 to 55% (40 to 60%) to the total Cameron band intensity when EUVAC (S2K) solar flux is used. The contribution of photodissociation of CO<sub>2</sub> to the IUE-observed Cameron band brightness is around 20% (30%) for EUVAC (S2K) solar flux model when the abundances of CO and CO<sub>2</sub> in the comet are almost equal. These computation show that in the IUE field of view the photoelectron is a major production source (60-75% contribution) for the Cameron band emission, whereas the contribution due to photons is small (20-35%).

The calculations presented in Tables 2 and 3 renders that in case of comets where CO<sub>2</sub>/CO abundance ratio is closer to 1 or larger than 1, the emission intensity of Cameron band is mainly controlled by the abundance of CO in the inner cometary coma. The photoelectron impact excitation of CO is the main production mechanism for the production of Cameron band emission, but not the photodissociative excitation of CO<sub>2</sub> as suggested or assumed in earlier studies (Weaver et al., 1994; Weaver et al., 1997; Feldman et al., 1997). Thus, in comets that have sufficient CO abundance the electron impact excitation of CO producing CO(a<sup>3</sup>Π) can be an efficient excitation mechanism for Cameron band emission. Since Cameron emission is mainly governed by electron impact excitation reactions, this emission can be used to track the photoelectron density mainly in the energy range 10 to 15 eV near the nucleus.

In the case of comet 103P/Hartley 2, which has an order of magnitude lower gas production rate and much lower CO (abundance < 1%) than comet 1P/Halley, the dissociative recombination of CO<sub>2</sub><sup>+</sup> becomes a competing production mechanism at larger ( $>10^4$  km) cometocentric distances (Bhardwaj and Raghuram, 2011a). However, in comparison, on comet 1P/Halley the production rates of H<sub>2</sub>O, CO<sub>2</sub>, and CO are so high that the photon and photoelectron impact reactions are dominant throughout the inner cometary coma.

### 3.2. Effect of electron impact cross section

In this section we will discuss the impact of cross sections for electron impact excitation of CO(a<sup>3</sup>Π) from CO<sub>2</sub> and CO. The threshold for exciting CO molecule in the metastable a<sup>3</sup>Π state is 6 eV and the peak value of cross section occurs around 10 eV (cf. Fig. 2). The cross section for electron impact excitation of CO producing CO(a<sup>3</sup>Π) reported by Jackman et al. (1977) is theoretically fitted based on Born approximation and experimental measurements of Ajello (1971). The uncertainty associated with measurement is about 75%. However, the uncertainty in the cross section at energies less than 15 eV is 35% (Ajello, 1971), where the contribution of

electron impact excitation plays a major role (cf. Fig 2). The cross section measurements of Furlong and Newell (1996) differ at the peak value of cross section by a factor 2 (cf. Figure 2). The threshold for dissociation of  $\text{CO}_2$  molecule into  $\text{CO}(\text{a}^3\Pi)$  state is 11.45 eV. Ajello (1971) measured Cameron band emission cross sections in the wavelength region 1950–2500 Å by exciting  $\text{CO}_2$  molecule through electron impact. Sawada et al. (1972) concluded that these cross sections are comparable with cross sections of 12.6 eV and 13.6 eV states. The cross section value for  $\text{CO}(\text{a}^3\Pi)$  production due to electron impact of  $\text{CO}_2$  measured at 80 eV by Erdman and Zipf (1983) is  $2.4 \times 10^{-16} \text{ cm}^2$ . Bhardwaj and Jain (2009) modified the fitting parameters given by Jackman et al. (1977) for the excited states 12.6 eV and 13.6 eV of  $\text{CO}_2$  molecule to match cross section value measured by Erdman and Zipf (1983) at 80 eV (for more discussion on these cross sections see Ajello, 1971; Sawada et al., 1972; Bhardwaj and Jain, 2009). Avakyan et al. (1998) corrected Ajello (1971) reported cross sections based on measurements of Erdman and Zipf (1983). The difference in the cross section of Avakyan et al. (1998) and Bhardwaj and Jain (2009) below 30 eV is about a factor of 2 (cf. Fig 2).

Using electron impact  $\text{CO}(\text{a}^3\Pi)$  excitation cross sections from Furlong and Newell (1996) for CO and from Avakyan et al. (1998) for  $\text{CO}_2$ , and using EUVAC solar flux, the calculated emission intensity of 1-0 Cameron band, for a given relative abundances of CO and  $\text{CO}_2$ , is larger by a factor 2. In these calculations the contribution of electron impact excitation of CO is increased from 70% to 85% at cometocentric distances below  $10^3$  km and 40% to 60% at distances above  $10^3$  km. On using these cross sections, the percentage contribution of photoelectron impact excitation of CO to the total Cameron emission in the IUE-slit-averaged intensity is found to increase by 10%, but there is no significant change in electron impact excitation of  $\text{CO}_2$ . In this case the contribution from photodissociative excitation of  $\text{CO}_2$  is decreased by 10%.

#### 4. Summary

Using the coupled chemistry-emission model a detailed study of Cameron band ( $\text{a}^3\Pi \rightarrow \text{X}^1\Sigma^+$ ) emission has been carried out on the comet 1P/Halley around the Giotto encounter period. The effects of change in solar flux on the production of  $\text{CO}(\text{a}^3\Pi)$  and thus the Cameron band intensity have been evaluated by considering two different solar EUV flux models, viz. EUVAC model (Richards et al., 1994) and S2K (SOLAR2000)

model (Tobiska, 2004). Calculations are made for different days of IUE-observation of comet 1P/Halley. The important results from the present model calculations can be summarized as follows:

- For the same day, the solar flux from the two models (EUVAC & S2K) are different, and the difference between them varies with wavelength.
- The production rates obtained by using S2K solar flux model are higher than that of EUVAC model. The photodissociation of  $\text{CO}_2$  is larger by a factor of 2.5, while the photoelectron impact excitation is larger by a factor of  $\sim 1.5$ .
- The total production rate of  $\text{CO}(\text{a}^3\Pi)$  peaks around cometocentric distance of 20 km for both solar flux models.
- Throughout the inner coma the main loss mechanism of  $\text{CO}(\text{a}^3\Pi)$  is radiative decay. Very close to the nucleus ( $< 20$  km) quenching by water is also significant.
- In the inner ( $\leq 5000$  km) coma the major production mechanism of  $\text{CO}(\text{a}^3\Pi)$  is photoelectron impact excitation of CO.
- On using EUVAC solar flux, and abundances of CO and  $\text{CO}_2$  as derived from IUE-observation, the model calculated Cameron band 1-0 emission intensity (40 R) is consistent with the IUE-observed brightness ( $37 \pm 6$  R) on 13 March 1986, and also on other days of observations. However, the calculated intensities are larger by a factor 1.5 when the S2K solar EUV flux is used.
- For EUVAC (S2K) solar flux model, around 70% (65%) of the total intensity of Cameron band observed by the IUE is contributed by electron impact excitation of CO and  $\text{CO}_2$  molecules, while the contribution from photodissociative excitation of  $\text{CO}_2$  is about 20–30% only.
- In comets having comparable CO and  $\text{CO}_2$  relative abundances, the intensity of Cameron band is largely determined by the photoelectron impact excitation of CO, and not the photodissociative excitation of  $\text{CO}_2$  as suggested by earlier studies.
- Since the emission intensity of Cameron band is mainly governed by electron impact reactions, this emission may be more useful to track the photoelectron density in 10–15 eV energy region in the inner coma, rather than the  $\text{CO}_2$  abundance.

## Acknowledgements

One of the authors (SR) was supported by ISRO research fellowship during the period of this study.

## References

- Ajello, J. M., 1971. Emission cross sections of CO<sub>2</sub> by electron impact in the interval 1260–4500 Å, II. *J. Chem. Phys.* 55, 3169–3177. doi: 10.1063/1.1676564.
- Avakyan, S. V., Il'in, R. N., Lavrov, V. M., Ogurtsov, G. N. (Eds.), 1998. *Collision Processes and Excitation of UV Emission from Planetary Atmospheric Gases: A Handbook of Cross Sections*. Gordon and Breach Science Publishers.
- Bhardwaj, A., 1999. On the role of solar EUV, photoelectrons, and auroral electrons in the chemistry of C(<sup>1</sup>D) and the production of CI 1931 Å in the inner cometary coma: A case for comet P/Halley. *J. Geophys. Res.* 104, 1929 – 1942. doi:10.1029/1998JE900004.
- Bhardwaj, A., 2003. On the solar EUV deposition in the inner coma of comets with large gas production rates. *Geophys. Res. Lett.* 30 (24). doi:10.1029/2003GL018495.
- Bhardwaj, A., Singhal, R. P., 1993. Optical thin H Lyman alpha production on outer planets: low energy proton acceleration in parallel electric fields and neutral H atom precipitation from ring current. *J. Geophys. Res.* 9473–9481 (98). doi:10.1029/92JA02400.
- Bhardwaj, A., Haider, S. A., Singhal, R. P., 1990. Auroral and photoelectron fluxes in cometary ionospheres. *Icarus* 85, 216 – 228. doi:10.1016/0019-1035(90)90112-M.
- Bhardwaj, A., Haider, S. A., Singhal, R. P., 1996. Production and emissions of atomic carbon and oxygen in the inner coma of comet 1P/Halley: Role of electron impact. *Icarus* 120, 412 – 430. doi: 10.1006/icar.1996.0061.
- Bhardwaj, A., Jain, S. K., 2009. Monte Carlo model of electron energy degradation in a CO<sub>2</sub> atmosphere. *J. Geophys. Res.* 114, 11309. doi:10.1029/2009JA014298; correction doi:10.1029/2009JA014298.
- Bhardwaj, A., Michael, M., 1999a. Monte Carlo model for electron degradation in SO<sub>2</sub> gas: Cross sections, yield spectra and efficiencies. *J. Geophys. Res.* 104 (10), 24713–24728. doi: 10.1029/1999JA900283.
- Bhardwaj, A., Michael, M., 1999b. On the excitation of Io's atmosphere by the photoelectrons: Application of the analytical yield spectrum of SO<sub>2</sub>. *Geophys. Res. Lett.* 26, 393 – 396. doi: 10.1029/1998GL900320.
- Bhardwaj, A., Raghuram, S., 2011a. Model for Cameron-band emission in comets: A case for the EPOXI mission target comet 103P/Hartley 2. *Mon. Not. R. Astron. Soc.* 412, L25 – L29. doi: 10.1111/j.1745-3933.2010.00998.x.
- Bhardwaj, A., Raghuram, S., 2011b. Coupled Chemistry-Emission Model for Atomic Oxygen Green and Red-doublet Emissions in Comets: A case study for the comet C/1996 B2 Hyakutake. *Astrophys. J.* (Submitted).
- Boice, D. C., Huebner, W. F., Keady, J. J., Schmidt, H. U., Wegmann, R., 1986. A model of comet P/Giacobini-Zinner. *Geophys. Res. Lett.* 13, 381–384. doi:10.1029/GL013i004p00381.
- Campbell, L., Brunger, M. J., 2009. Electron impact excitation of the carbon monoxide in comet Hale-Bopp. *Geophys. Res. Lett.* 36. doi:10.1029/2008GL036641.
- Cravens, T. E., Green, A. E. S., 1978. Airglow from the inner comas of comets. *Icarus* 33, 612–623. doi:10.1016/0019-1035(78)90193-8.
- Conway, R. R., 1981. Spectroscopy of the Cameron bands in the Mars airglow. *J. Geophys. Res.* 86, 4767 – 4775. doi: 10.1029/JA086iA06p04767.
- Cottin, H., Fray, N., 2008. Distributed sources in comets. *Space Sci. Rev.* doi:10.1007/s11214-008-9399-z.
- DiSanti, M., Mumma, M., Russo, N. D., Magee-Sauer, K., Griep, D., 2003. Evidence for a dominant native source of carbon monoxide in comet C/1996 B2 (Hyakutake). *J. Geophys. Res. Planets* 108f, 15–11. doi:10.1007/s11214-008-9399-z.
- Eberhardt, P., 1999. Distributed sources in comets. *Space Science Rev.* 90, 45–52. doi:10.1023/A:1005221309219.
- Eberhardt, P., Krankowsky, D., Schulte, W., Dolder, U., Lammerzähl, P., Berthelier, J. J., Woweries, J., Stubbemann, U., Hodges, R. R., Hoffman, J. H., Illiano, J. M., 1987. The CO and N<sub>2</sub> Abundance in Comet 1P/Halley. *Astron. Astrophys.* 187, 481–414.
- Erdman, P. W., Zipf, E. C., 1983. Electron-impact excitation of the Cameron system ( $a^3\Pi \rightarrow X^1\Sigma$ ) of CO. *Planet. Space Sci.* 31, 317 – 321. doi:10.1016/0032-0633(83)90082-X.
- Feldman, P. D., Cochran, A. L., Combi, M. R., 2004. Spectroscopic investigations of fragment species in the coma: in comets II. M. C. Festou, H. A. Weaver, & H. U. Keller (Ed.) (Tucson: Univ. of Arizona).
- Feldman, P. D., Festou, M. C., Tozzi, G. P., Feldman, P. D., Weaver, H. A., 1997. The CO<sub>2</sub>/CO abundance ratio in 1P/Halley and several other comets observed by IUE and HST. *Astrophys. J.* 475, 829–834. doi:10.1086/303553.
- Feldman, P. D., Lupu, R. E., McCandliss, S. R., Weaver, H. A., 2009. The far ultraviolet spectral signatures of formaldehyde and carbon dioxide in comets. *Astrophys. J.* 699 (2), 1104–1112. doi: 10.1088/0004-637X/699/2/1104.
- Festou, M. C., 1999. Distributed sources in comets. *Space Science Rev.* 90, 53 – 67. doi:10.1023/A:1005225426057.
- Furlong, J. M., Newell, W. R., 1996. Total cross section measurement for the metastable ( $a^3\Pi$ ) state in CO. *J. Phys. B: At. Mol. Phys.* 29, 331 – 338. doi:10.1088/0953-4075/29/2/020.
- Gilijamse, J. J., Hoekstra, S., Meek, S. A., Metsälä, M., van de Meerakker, S. Y. T., T. S. Y., Meijer, G., Groenenboom, G. C., C., G., 2007. The radiative lifetime of metastable CO ( $a^3\Pi, \nu=0$ ). *J. Chem. Phys.* 127, 221102–4. doi:10.1063/1.2813888.
- Greenberg, J. M., Li, A., 1998. From interstellar dust to comets: the extended CO source in Halley. *Astron. Astrophys.* 332, 374 – 384.
- Häberli, R. M., Altwegg, K., Balsiger, H., Geiss, J., 1996. Heating of the thermal electrons in the coma of comet P/Halley. *J. Geophys. Res.* 101 (A7), 15579–15589.
- Haider, S. A., Bhardwaj, A., 2005. Radial distribution of production rates, loss rates and densities corresponding to ion masses  $\leq 40$  amu in the inner coma of comet Halley: Composition and chemistry. *Icarus* 177, 196 – 216. doi:10.1016/j.icarus.2005.02.019.
- Haider, S. A., Bhardwaj, A., Singhal, R. P., 1993. Role of auroral and photoelectrons on the abundances of Methane and Ammonia in the coma of comet Halley. *Icarus* 101, 234 – 243. doi: 10.1006/icar.1993.1021.
- Huebner, W. F., Keady, J. J., Lyon, S. P., 1992. Solar photorates for planetary atmospheres and atmospheric pollutants. *Astrophys. Space Sci.* 195 (1), 1–294. doi:10.1007/BF00644558.
- Ip, W., 1985. A preliminary consideration of the electron impact ionization effect in cometary comas. *Adv. Space Res.* 5, 47–51. doi: 10.1016/0273-1177(85)90066-3.
- Itikawa, Y., Mason, N., 2005. Cross sections for electron collisions with water molecules. *J. Phys. Chem. Ref. Data* 34 (1), 1–22. doi: 10.1063/1.1799251.
- Jackman, C. H., Garvey, R. H., Green, A. E. S., 1977. Electron impact on atmospheric gases, I, updated cross sections. *J. Geophys. Res.* 82, 5081–5090. doi:10.1029/JA082i032p05081.
- Körösmeszey, A., Cravens, T. E., Gombosi, T. I., Nagy, A. F., Mendis, D. A., Szegő, K., Gribov, B. E., Sagdeev, R. Z., Shapiro, V. D., Shevchenko, V. I., 1987. A new model of cometary ionosphere. *J. Geophys. Res.* 92 (A7), 7331 – 7340. doi:



- 10.1029/JA092iA07p07331.
- Krankowsky, D., Lammerzahl, P., Herrwerth, I., Woweries, J., Eberhardt, P., Dolder, U., Herrmann, U., Schulte, W., Berthelier, J. J., Illiano, J. M., Hodges, R. R., Hoffman, J. H., 1986. In situ gas and ion measurements at comet Halley. *Nature* 321, 326–329. doi: 10.1038/321326a0.
- Lawrence, G. M., 1972. Photodissociation of  $\text{CO}_2$  to produce  $\text{CO}(\text{a}^3\pi)$ . *J. Chem. Phys.* 56 (7), 3435 – 3442. doi: 10.1063/1.1677717.
- McConkey, J. W., Malone, C. P., Johnson, P. V., Winstead, C., McKoy, V., Kanik, I., 2008. Electron impact dissociation of oxygen-containing molecules A critical review. *Phys. Rept.* 466, 1–103. doi:10.1016/j.physrep.2008.05.001.
- McCormick, P. T., Michelson, P. F., Pettibone, D. W., Whitten, R. C., 1976. On the energy deposition of photoelectrons in the atmosphere of Venus. *J. Geophys. Res.* 81, 5196 – 5200. doi: 10.1029/JA081i028p05196.
- Nicholls, R. W., 1962. Laboratory astrophysics. *J. Quant. Spectry. Radiat. Transfer* 2, 433 – 449. doi:10.1016/0022-4073(62)90030-4.
- Rao, M. V. V. S., Iga, I., Srivastava, S. K., 1995. Ionization cross-sections for the production of positive ions from  $\text{H}_2\text{O}$  by electron impact. *J. Geophys. Res.* 100, 26421–26425. doi: 10.1029/95JE02314.
- Richards, P. G., Fennelly, J. A., Torr, D. G., 1994. EUVAC: A solar EUV flux model of aeronomic calculations. *J. Geophys. Res.* 99 (A5), 8981–8992. doi:10.1029/94JA00518.
- Rosati, R. E., Johnsen, R., Golde, M. F., 2003. Absolute yields of  $\text{CO}(\text{a}^3\Sigma^+, \text{d}^3\Delta_g, \text{e}^3\Sigma^-) + \text{O}$  from the dissociative recombination of  $\text{CO}_2^+$  ions with electrons. *J. Chem. Phys.* 119 (22), 11630–11635. doi:10.1063/1.1623480.
- Rosati, R. E., Skrzypkowski, M. P., Johnsen, R., Golde, M. F., 2007. Yield of excited CO molecules from dissociative recombination of  $\text{HCO}^+$  and  $\text{HOC}^+$  ions with electrons. *J. Chem. Phys.* 126, 154302. doi:10.1063/1.2715943.
- Sawada, T., Strickland, D. J., Green, A. E. S., 1972. Electron energy deposition in  $\text{CO}_2$ . *J. Geophys. Res.* 77, 4812 – 4818. doi: 10.1029/JA077i025p04812.
- Schmidt, H. U., Wegmann, R., Huebner, W. F., Boice, D. C., 1988. Cometary gas and plasma flow and with detailed chemistry. *Comp. Phys. Comm.* 49, 17 – 59. doi:10.1016/0010-4655(88)90214-7.
- Seiersen, K., Al-Khalili, A., Heber, O., Jensen, M. J., Nielsen, I. B., Pedersen, H. B., Safvan, C. P., Andersen, L. H., 2003. Dissociative recombination of the cation and dication of  $\text{CO}_2$ . *Phys. Rev. A* 68. doi:10.1103/PhysRevA.68.022708.
- Shunk, R. W., Nagy, A. F., 2009. *Ionospheres - physics, plasma physics, and chemistry*. Cambridge University Press.
- Singhal, R. P., Bhardwaj, A., 1991. Monte Carlo Simulation of Photoelectron Energization in Parallel Electric Fields: Electrogrow on Uranus. *J. Geophys. Res.* 96, 15963 – 15972.
- Singhal, R. P., Haider, S. A., 1984. Analytical yield spectrum approach to photoelectron fluxes in the earth's atmosphere. *J. Geophys. Res.* 89, 6847–6852. doi:10.1029/JA089iA08p06847.
- Skrzypkowski, M. P., Gougousi, T., Johnsen, R., Golde, M. F., 1998. Measurement of the absolute yield of  $\text{CO}(\text{a}^3\pi) + \text{O}$  products in the dissociative recombination of  $\text{CO}_2^+$  ions with electrons. *J. Chem. Phys.* 108 (20), 8400 – 8407. doi:10.1063/1.476267.
- Tobiska, W. K., 2004. SOLAR2000 irradiances for climate change, aeronomy and space system engineering. *Adv. Space Res.* 34, 1736 – 1746. doi:10.1016/j.asr.2003.06.032.
- Tozzi, G. P., Feldman, P. D., Festou, M. C., 1998. Origin and production of  $\text{C}(\text{I}^1\text{D})$  atoms in cometary comae. *Astron. Astrophys.* 330, 753–763.
- Weaver, H. A., Feldman, P. D., A'Hearn, M. F., Arpigny, C., Brandt, J. C., Festou, M. C., Haken, M., McPhate, J. B., Stern, S. A., Tozzi, G. P., 1997. The activity and size of the nucleus of comet Hale-Bopp (C/1995 O1). *Science* 275, 1900–1904.
- Weaver, H. A., Feldman, P. D., McPhate, J. B., A'Hearn, M. F., Arpigny, C., Smith, T. E., 1994. Detection of CO Cameron band emission in comet P/Hartley-2 (1991 XV) with the Hubble Space Telescope. *Astrophys. J.* 422, 374 – 380. doi:10.1086/173732.
- Wysong, I. J., 2000. Measurement of quenching rates of  $\text{CO}(\text{a}^3\Pi)$  using laser pump and probe technique. *Chem. Phys. Lett.* 1 - 2, 42 – 46. doi:10.1016/S0009-2614(00)00967-2.

Table 1: Reactions for the production and loss of CO( $a^3\Pi$ ).

Reaction	Rate( $\text{cm}^3 \text{ s}^{-1}$ or $\text{s}^{-1}$ )	Reference
$\text{CO}_2 + h\nu \rightarrow \text{CO}(a^3\Pi) + \text{O}(^3\text{P})$	Model	<i>Present work</i>
$\text{CO} + h\nu \rightarrow \text{CO}(a^3\Pi)$	$1.69 \times 10^{-9}$	Weaver et al. (1994)
$\text{CO}_2 + e_{ph}^- \rightarrow \text{CO}(a^3\Pi) + \text{O} + e^-$	Model	<i>Present work</i>
$\text{CO} + e_{ph}^- \rightarrow \text{CO}(a^3\Pi) + e^-$	Model	<i>Present work</i>
$\text{CO}_2^+ + e^- \rightarrow \text{CO}(a^3\Pi) + \text{O}$	$K_a^*$	Seiersen et al. (2003), Rosati et al. (2003)
$\text{HCO}^+ + e^- \rightarrow \text{CO}(a^3\Pi) + \text{H}$	$K_b^\dagger$	Rosati et al. (2007), Schmidt et al. (1988)
$\text{CO}(a^3\Pi) + h\nu \rightarrow \text{C} + \text{O}$	$7.2 \times 10^{-5}$	Huebner et al. (1992)
$\text{CO}(a^3\Pi) + h\nu \rightarrow \text{CO}^+ + e^-$	$8.58 \times 10^{-6}$	Huebner et al. (1992)
$\text{CO}(a^3\Pi) + h\nu \rightarrow \text{O} + \text{C}^+ + e^-$	$2.45 \times 10^{-8}$	Huebner et al. (1992)
$\text{CO}(a^3\Pi) + h\nu \rightarrow \text{C} + \text{O}^+ + e^-$	$2.06 \times 10^{-8}$	Huebner et al. (1992)
$\text{CO}(a^3\Pi) + \text{H}_2\text{O} \rightarrow \text{CO} + \text{H}_2\text{O}$	$3.3 \times 10^{-10}$	Wysong (2000)
$\text{CO}(a^3\Pi) + \text{CO}_2 \rightarrow \text{CO} + \text{CO}_2$	$1.0 \times 10^{-11}$	Skrzypkowski et al. (1998)
$\text{CO}(a^3\Pi) + \text{CO} \rightarrow \text{CO} + \text{CO}$	$5.7 \times 10^{-11}$	Wysong (2000)
$\text{CO}(a^3\Pi) + e_{ph}^- \rightarrow \text{CO}^+ + 2e^-$	Model	<i>Present work</i>
$\text{CO}(a^3\Pi) \rightarrow \text{CO} + h\nu$	$1.26 \times 10^2$	Lawrence (1972)

\*  $K_a = 6.5 \times 10^{-7} (300/\text{Te})^{0.8} \times 0.87 \times 0.29 \text{ cm}^3 \text{ s}^{-1}$ ; here 0.87 is yield of dissociative recombination of  $\text{CO}_2^+$  producing CO, and 0.29 is yield of  $\text{CO}(a^3\Pi)$  produced from CO.

$\dagger K_b = 2.4 \times 10^{-7} (300/\text{Te})^{0.7} \times 0.23 \text{ cm}^3 \text{ s}^{-1}$ ; here 0.23 is yield of dissociative recombination of  $\text{HCO}^+$  producing  $\text{CO}(a^3\Pi)$ ,  $e_{ph}^-$  = photoelectron.

Table 2: Calculated brightness of the Cameron band at comet 1P/Halley for different conditions on 13 March 1986.

Relative abundance (%)		IUE-slit averaged brightness (R)		Percentage contribution to total Cameron band for different processes at three different projected radial distances (km)										Total Cameron band brightness (R)		
				hν + CO <sub>2</sub>			e <sup>-</sup> + CO <sub>2</sub>			e <sup>-</sup> + CO						
CO <sub>2</sub>	(%)	(1-0)*	(0-0)	(0-1)	10 <sup>2</sup>	10 <sup>3</sup>	10 <sup>4</sup>	10 <sup>2</sup>	10 <sup>3</sup>	10 <sup>4</sup>	10 <sup>2</sup>	10 <sup>3</sup>	10 <sup>4</sup>	IUE-slit averaged	Height integrated column	
EUVAC	4	59	44	63	9	14	52	15	15	15	11	74	66	25	2	5
	4	51	38	54	9	15	65	14	16	13	13	75	64	12	3	5
	3	46	34	48	7	12	63	11	13	12	80	70	70	15	2	5
	4.3	45	34	48	11	19	69	20	21	13	68	55	55	9	0.5	3
S2K	4	87	66	96	14	19	61	13	13	13	9	71	62	20	0.5	3
	4	77	58	82	14	21	73	13	14	10	10	71	60	10	0.5	2
	3	68	51	72	11	17	71	10	12	9	77	66	66	11	0.5	2
	4.3	67	50	70	16	24	76	17	18	10	65	52	52	6	0.5	3

\*The intensity of Cameron (1-0) band observed by IUE is 37±6 Raleighs on 13 March 1986.; †Ext: Extended CO distribution.; e<sup>-</sup> is photoelectron and e<sup>-</sup> is thermal electron.;

Table 3: Calculated brightness of the Cameron band at comet 1P/Halley on different days of IUE observations.

Date in March 1986 EUVAC	r (AU)	$\Delta$ (AU)	$Q_{H_2O}$ ( $10^{29}$ $s^{-1}$ ) <sup>†</sup>	Derived abundances $\frac{abundance_{CO}}{abundance_{CO_2}}$ <sup>‡</sup>	Ratio $\frac{Q_{CO_2}}{Q_{CO}}$	IUE-slit averaged brightness			Percentage contribution to the IUE-slit averaged total Cameron band emission for different excitation processes (%)				IUE-slit averaged total brightness (R)
						(1-0) (R)	(0-0)	(0-1)	$h\nu + CO_2$	$e_{ph}^- + CO_2$	$e_{ph}^- + CO$	$e^- + CO_2^+$	
9	0.84	1.07	7.50	6.0	0.92	75 [64 $\pm$ 9] <sup>*</sup>	57	80	22	22	51	3	550
11	0.87	1.02	5.84	5.1	1.2	43 [43 $\pm$ 8]	32	45	25	24	44	4	310
13	0.90	0.96	5.98	4.3	0.9	40 [37 $\pm$ 6]	30	43	22	21	51	4	293
16	0.95	0.89	4.90	6.3	0.77	42 [44 $\pm$ 9]	32	45	23	20	51	4	307
18	0.97	0.84	4.92	2.8	0.68	24 [20 $\pm$ 6]	18	26	20	19	57	3	177
S2K													
9	0.84	1.07	7.50	6.0	0.92	116 [64 $\pm$ 9]	87	123	31	19	44	4	837
11	0.87	1.02	5.84	5.1	1.2	66 [43 $\pm$ 8]	49	69	33	21	39	4	475
13	0.90	0.96	5.98	4.3	0.9	62 [37 $\pm$ 6]	46	65	30	19	45	4	446
16	0.95	0.89	4.90	6.3	0.77	64 [44 $\pm$ 9]	48	68	30	18	45	4	456
18	0.97	0.84	4.92	2.8	0.68	37 [20 $\pm$ 6]	28	39	25	16	53	3	262

<sup>\*</sup>The value in square brackets is IUE-observed (1-0) Cameron band intensity;  $e_{ph}^-$  = photoelectron,  $e^-$  = thermal electron. <sup>†</sup>The production rates of H<sub>2</sub>O and abundances of CO<sub>2</sub> & CO are taken from Feldman et al. (1997).

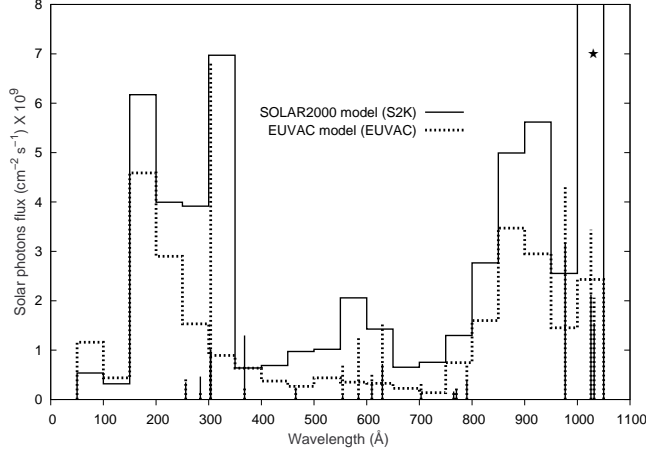


Figure 1: Solar EUV fluxes from EUVAC model (Richards et al., 1994) and SOLAR2000 (S2K) model (Tobiska, 2004) for the day 13 March 1986. Significant differences in the two model solar EUV fluxes can be noticed. (★) The value of solar flux in SOLAR2000 model for the bin 1000–1050 Å is  $30 \times 10^9 \text{ cm}^{-2} \text{ s}^{-1}$ .

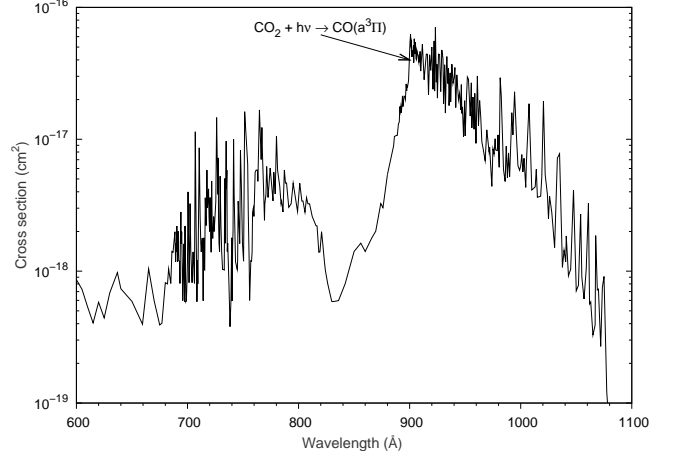


Figure 3: Photodissociative excitation cross section of  $\text{CO}_2$  producing  $\text{CO}(\text{a}^3\Pi)$ , taken from Huebner et al. (1992).

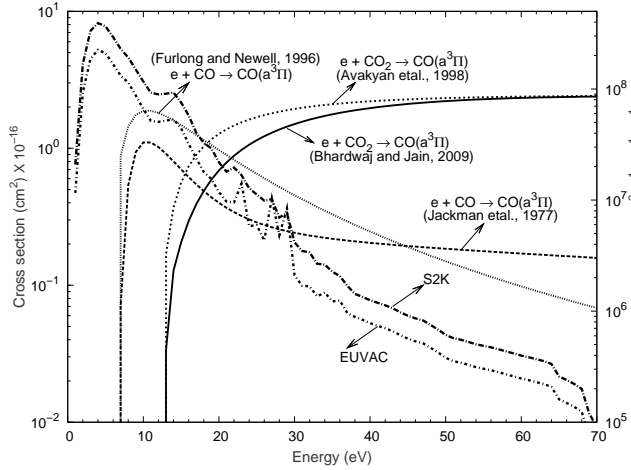


Figure 2: Cross sections for electron impact excitation of  $\text{CO}(\text{a}^3\Pi)$  from  $\text{CO}$  and  $\text{CO}_2$ . Calculated photoelectron flux at cometocentric distance of 1000 km is also shown for both SOLAR2000 (S2K) and EUVAC model solar fluxes with magnitude on right side y-axis

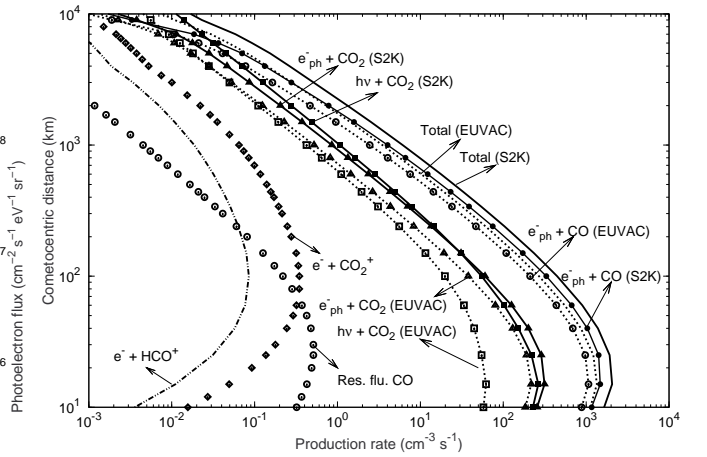


Figure 4: Radial profiles of various production mechanisms of  $\text{CO}(\text{a}^3\Pi)$  in comet 1P/Halley on 13 March 1986 for relative abundance of 4%  $\text{CO}_2$  and 7%  $\text{CO}$ . The calculated profiles for dissociative recombination of  $\text{CO}_2^+$  and  $\text{HCO}^+$ , and resonance fluorescence of  $\text{CO}$  are shown for EUVAC solar flux only. Res. flu. = resonance fluorescence of  $\text{CO}$  molecule.  $e_{ph}^-$  = Photoelectron,  $h\nu$  = Solar photon, and  $e^-$  = thermal electron.

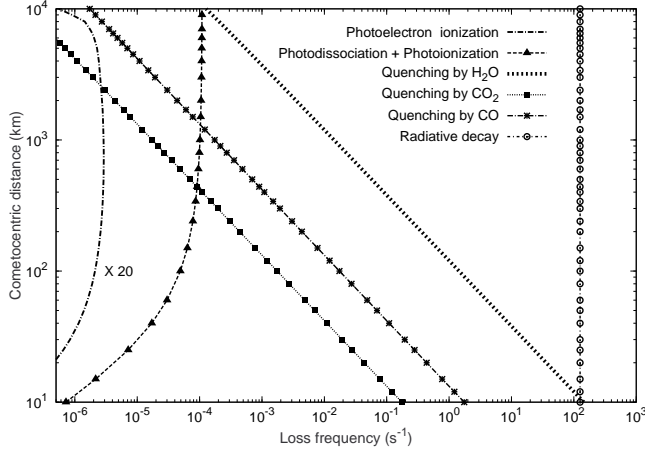


Figure 5: Radial profiles of various loss mechanisms of  $\text{CO}(a^3\Pi)$  for 4%  $\text{CO}_2$  and 7%  $\text{CO}$  relative abundances using EUVAC solar flux. Photoelectron impact ionization of  $\text{CO}(a^3\Pi)$  is plotted after multiplying by a factor 20.

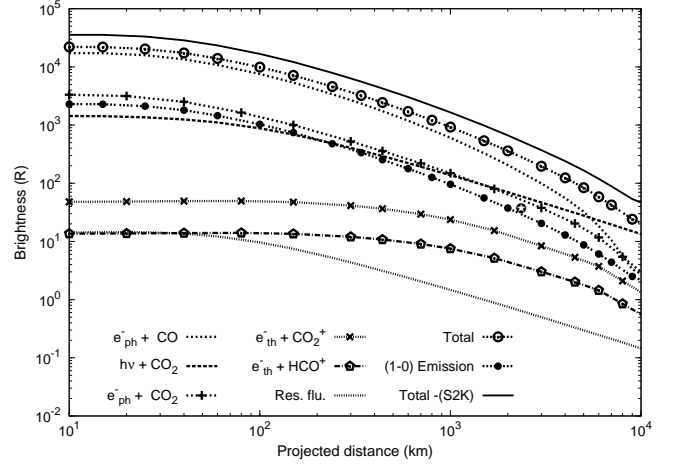


Figure 7: The integrated Cameron band brightness profiles as a function of projected distance from nucleus for different production processes of the Cameron band, using EUVAC solar flux model and relative contribution of 4%  $\text{CO}_2$  and 7%  $\text{CO}$ . The calculated brightness profiles for Cameron (1-0) band for EUVAC solar flux and total brightness for S2K solar flux are also shown.

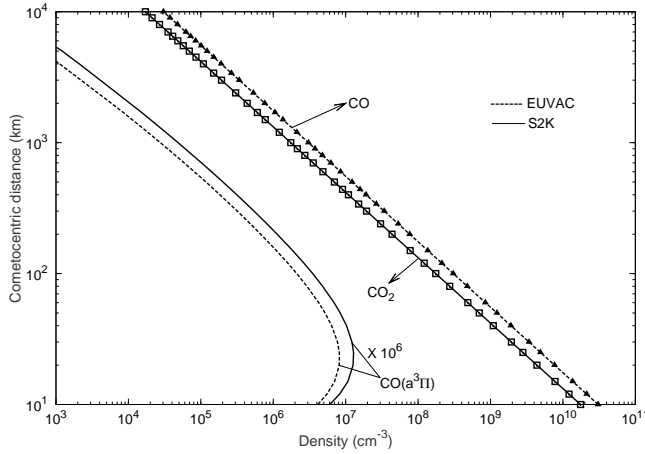


Figure 6: The calculated radial profiles of number density  $\text{CO}(a^3\Pi)$  for SOLAR2000 (S2K) and EUVAC solar flux models. The density of  $\text{CO}(a^3\Pi)$  is plotted after multiplying by a factor  $10^6$ . The number density profiles of  $\text{CO}_2$  and  $\text{CO}$  are also shown for 4% and 7% relative abundances, respectively.

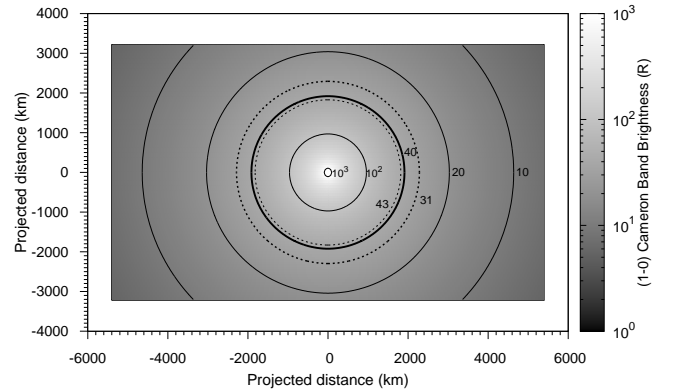


Figure 8: The calculated (1-0) Cameron band emission brightness in the IUE projected field of view on 13 March 1986, assuming spherical symmetry, using EUVAC solar flux model, for relative contribution of 4.3%  $\text{CO}_2$  and 4.7%  $\text{CO}$ . The rectangle represent the projected field of view corresponding to IUE slit dimension of  $9.07'' \times 15.1''$  centred on the nucleus of comet 1P/Halley, which is  $11000 \times 6600$  km. The gray scale represent the calculated brightness with contours (solid lines) for  $10^3$ ,  $10^2$ , 20, and 10 R marked in the figure. The calculated brightness averaged over IUE slit projected area (40 R) is shown by thick black contour between two dotted line contours which represent the upper and lower limits of IUE observed intensity value ( $37 \pm 6$  R).